Universidade do Minho
Escola de Ciências

Development of optical (T-LSPR) biosensors, based in nanoplasmonic thin films, for fast Legionella pneumophila detection in patients or environmental samples

Diogo Emanuel Carvalho Costa

Programa Doutoral em Física – MAP-fis

Ph.D. Progress Report

Supervisors:

Professor Filipe Vaz

Professor Paula Sampaio

Professor Graça Minas

January 2022

1. Introduction

Legionella is a Gram-negative bacterium present in freshwater habitats and that can colonize man-made water system [1] and can be dispersed by aerosols generated by showers, faucets, cooling towers, etc. [2]. *Legionella pneumophila* is responsible for more than 90% of cases of Legionnaires' disease and outbreaks of community-acquired and nosocomial *L. pneumophila* infection have been recently described in Portugal. While *L. pneumophila* have at least 16 serogroups, the serogroup 1 is responsible for most of the American and European clinical cases [3].

The detection of this pathogen from clinical or environment samples is mainly performed by culture plate methods, which takes up to 10 days [3]. The detection of *L. pneumophila* infections can also be executed using the urinary antigen test due to its simplicity, speed, and in-situ [4], however, this only detects the serogroup 1, producing a detection blind spot for the remaining serogroups [5].

Antibodies detection methods usually relies on the detection of pathogen' specific proteins and are used due to the low detection limit (103 CFU/mL). However, they are not appropriate for heat or chemically processed samples (e.g. water treatment stations). Furthermore, the Portuguese legal limit of *L. pneumophila* in the environment is 102 CFU/L (Portaria n°353-A/2013). Methods based on DNA stand as a viable alternative since their detection limit is already lower than protein-based methods [6]. Therefore, an alternative, highly sensitive and easy method with a short detection time is needed to improve patient's survival and prevent *L. pneumophila* outbreaks.

Localized Surface Plasmon Resonance (LSPR) has emerged as a capable technique in the field of label-free biosensing [7]. LSPR is associated with resonance of incident electromagnetic (EM) waves with collective oscillations at the interface of noble metal surfaces with a dielectric medium [8], leading to strong EM fields with an absorption band at a specific wavelength [9]. In LSPR sensing, these EM fields are sensitive to changes in the refractive index (RI) of the surrounding medium [10]. Due to the stronger EM field confinement, a smaller penetration of the evanescent field into the dielectric is observed [11], translating in an increase of sensitivity for RI changes near the nanoparticles' surface [12,13]. These characteristics are suitable for the development of a diagnostic tool to quickly detect biological entities whose detection with lower concentrations is crucial.

LSPR absorption band can be excited by the transmitted EM radiation, described as Transmission-LSPR (T-LSPR) [14,15], which can simplify the detection system, opening the possibility of constructing a miniaturized device [16].

However, the development and production of reliable T-LSPR platforms requires reproducible and stable optical properties [17]. Magnetron sputtered nanocomposite thin films, with noble nanoparticles embedded in a dielectric matrix [18], such as those composed of Au [19,20] or Ag [21] dispersed in a dielectric matrix, have already showed potential as T-LSPR platforms. The LSPR absorption band can be tuned by changing several deposition parameters [22] and post-deposition annealing treatments [23]. The Au/TiO_2 system has been a subject of intense research in the last years in the investigation group, and "optimized" conditions for its preparation have been reached [24].

Other critical issue in T-LSPR biosensors is functionalization of the nanoparticles with biorecognition elements [25], such as antibodies [26], aptamers [27] or even DNA [28]. These molecules are used to functionalize the sensor, leading to the immobilization of the analyte molecules near the nanoparticles' surface [10].

2. Results

2.1 Optimization of nanoplasmonic thin films with tailored Transmittance-LSPR (T-LSPR) bands

To produce sensible LSPR transducers from magnetron sputtered thin films, the titanium dioxide matrix was chosen, as it is the most studied in the nanoplasmonic sputtered thin films topic. As for the noble metal, gold and silver are the most researched metals in terms of plasmonic nanoparticles. Therefore, sets of TiO_2 sputtered thin films with embedded Au, Ag and Au-Ag nanoparticles were produced, to choose the best candidates to use in a LSPR biosensor system.

The general deposition parameters were similar throughout all produced systems, only changing the amount of noble metal placed on the erosion track of the titanium target, the applied current and deposition time. The base pressure was approximately 6.0×10^{-6} mbar, while the working pressure was 4.1×10^{-3} mbar. The argon and oxygen flows were 25 and 5 sccm, respectively. The substrate holder has rotating constantly at 5.5 rpm. The applied current was varied between 1.5 and 2.0 A, and the deposition time between 10 and 20 nm, corresponding to thin films with approximately 50 and 100 nm of thickness. To produced Au/TiO_2 and Ag/TiO_2 thin films, 1 or 2 pellets of Au or Ag were used. In the case of $Au\text{-}Ag/TiO_2$ thin films, three combinations of Au and Ag were used: ½ pellet of Au + ½ pellet of Ag, ½ pellet Au + ¼ pellet of Ag, and ½ pellet of Au + 1 pellet of Ag.

With this, a total of 28 different depositions were made, producing 8 thin films of Au/TiO_2 and 8 thin films of Ag/TiO_2 (for a total of 4 chemical composition each and 2 different thicknesses) and 12 thin films of $Au\text{-}Ag/TiO_2$, with 6 different chemical compositions and 2 different thicknesses.

Rutherford Backscattering Spectrometry (RBS) measurements were performed to confirm the chemical composition of the thin films, and the results are presented in the Table 1.

Table 1 – RBS results for the plasmonic thin films.

			Chemical composition (at. %)			
	Current (A)	Nobel metal pellets	Ti (±0.5 at.%)	O (±3 at.%)	Au (±0.5 at.%)	Ag (±0.5 at.%)
Au/TiO2	2	1 Au	18.03	69.33	12.73	0
	2	2 Au	16.27	66.22	17.57	0
	1,5	1 Au	16.51	65.57	19.22	0
	1,5	2 Au	16.21	55.36	27.68	0
Au/Ag-TiO2	2	1/2 Au + 1/2 Ag	25.06	54.5	7.86	11.82
	2	1/2 Au + 1 Ag	26.15	60.02	4.13	9.17
	2	1/2 Au + 1/4 Ag	24.26	67.77	3.68	3.69
	1,5	1/2 Au + 1/2 Ag	21.66	51.65	10.04	16.09
	1,5	1/2 Au + 1 Ag	20.3	52.52	10.29	18.42
	1,5	1/2 Au + 1/4 Ag	27.3	54.94	9.31	7.66
Ag/TiO2	2	1 Ag	20.46	56.83	0	22.13
	2	2 Ag	16.6	54.22	0	28.39
	1,5	1 Ag	20.51	54.62	0	24.2
	1,5	2 Ag	12.80	56.07	0	30.22

To promote nanoparticle formation and growth from the noble metals disperse in the TiO_2 matrix, post-deposition annealing was utilized. The temperatures chosen were 400 and 600 °C. 400 °C is below the melting point of glass, which would allow to create cheaper sensors. In the other hand, 600 °C was chosen because it promotes the growth of bigger nanoparticles, in comparison with 400 °C. No temperature was chosen above 600 °C because the formation of grooves due to the grain boundaries from the crystallization of TiO_2. These thermal treatments were performed in a vacuum furnace at 8 x 10^{-6} mbar, to insure no adsorption of O_2 by the thin films. Furthermore, previous studies showed the increase of thin film sensitivity to the surrounding media after Ar plasma etching. The plasma treatment was performed at 50 W for 30 min, with a working pressure of 0.8 mbar of Ar.

After annealing and plasma etching, the transmittance spectra of the thin films were measured to observe the LSPR band due to the formation and growth of the nanoparticles.

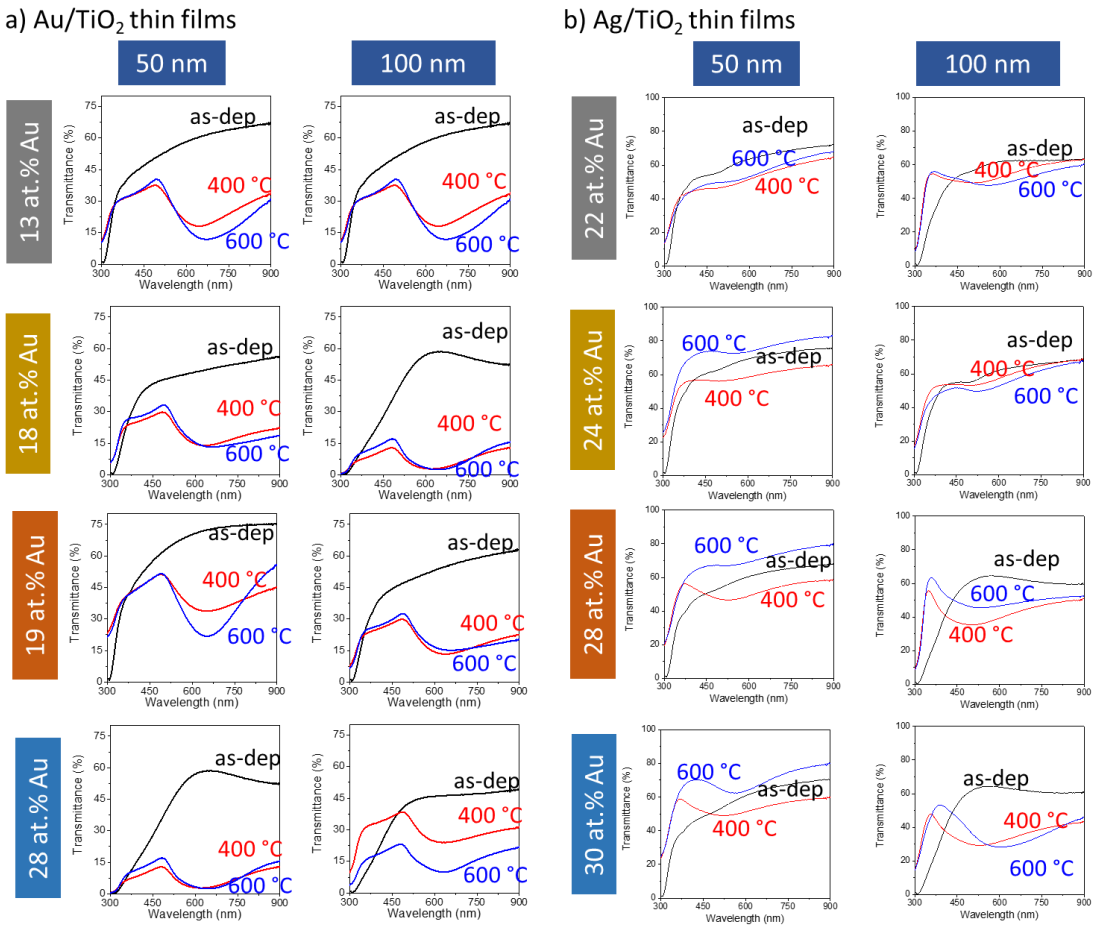

Figure 1 – Transmittance spectra for the LSPR bands for the plasmonic system: a) Au/TiO_2 and b) Ag/TiO_2.

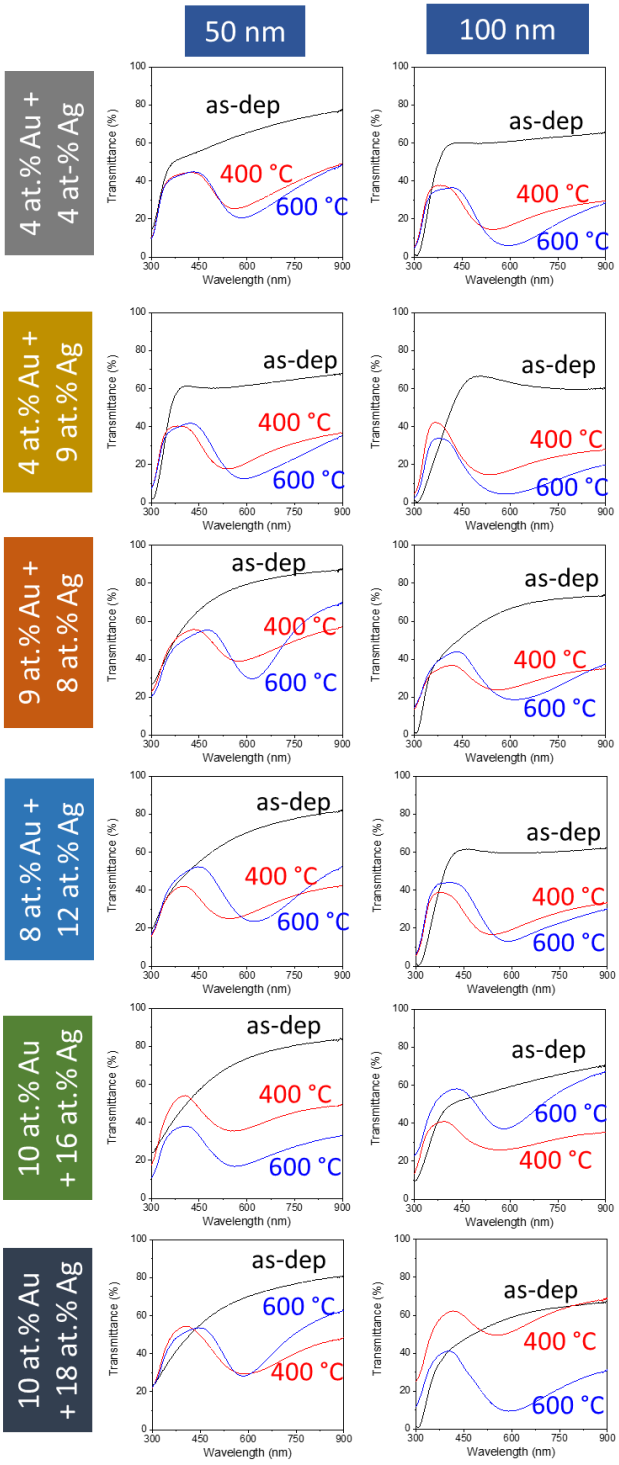

Figure 2 - Transmittance spectra for the LSPR bands for the bimetallic plasmonic system.

After optical characterization of the LSPR bands of the thin films, the refractive index sensitivity of each Au/TiO_2 and Au-Ag/TiO_2 were estimated. For this, the optical response of the thin films was measured using two media with different refractive indexes: deionized water (η= 1.3325 RIU) and a 20% (w/w) sucrose solution (η= 1.3639 RIU). The resulting spectra were analyzed using NANOPTICS software and this allowed to estimate the RIS for each thin film [29]. However, due to limitations of the optical system (the spectrophotometer was highly sensitive for wavelengths between 420 and

720 nm), some samples are excluded due to the RIS estimate, due to their LSPR bands characteristics (low intensity of the higher wavelengths tail.

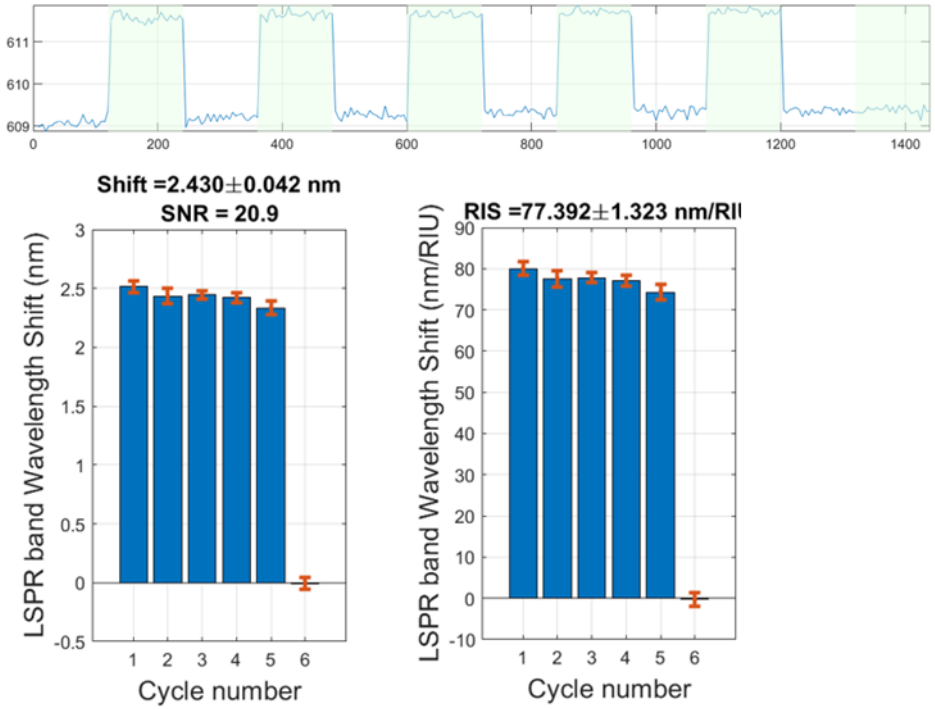

Figure 4 – Example of the results obtain for the plasmonic thin films in NANOPTICS software.

After analysis with NANOPTICS, the resulting RIS values were compiled in the table that follows (Table 2).

Table 2 – RIS values for the Au/TiO_2 thin films throughout all compositions, thicknesses, and annealing temperatures.

	Chemical composition	Thickness (nm)	Annealing temperature (°C)	RIS ($nm.RIU^{-1}$)
Au/TiO_2	13 at. % Au	50	400	-
			600	25 ± 7
		100	400	17 ± 3
			600	-
	18 at. % Au	50	400	28 ± 5
			600	-
		100	400	58 ± 12
			600	15 ± 2
	19 at. % Au	50	400	-
			600	-
		100	400	-
			600	55 ± 11
	28 at. % Au	50	400	25 ± 10
			600	22 ± 12
		100	400	13 ± 5
			600	77 ± 1

Table 3 – RIS values for the Au-Ag/TiO_2 thin films throughout all compositions, thicknesses, and annealing temperatures.

	Chemical composition	Thickness (nm)	Annealing temperature (°C)	RIS (nm.RIU-1)
Au-Ag/TiO_2	4 at.% Au + 4 at-% Ag	50	400	-110 ± 3
			600	-33 ± 2
		100	400	-
			600	-82.2 ± 0.9
	4 at.% Au + 9 at.% Ag	50	400	24 ± 7
			600	-
		100	400	32 ± 3
			600	23 ± 1
	9 at.% Au + 8 at.% Ag	50	400	250 ± 18
			600	-16 ± 1
		100	400	96 ± 9
			600	-
	8 at.% Au + 12 at.% Ag	50	400	53 ± 4
			600	-
		100	400	36 ± 2
			600	5 ± 2
	10 at.% Au + 16 at.% Ag	50	400	-245 ± 58
			600	29± 4
		100	400	-
			600	-
	10 at.% Au + 18 at.% Ag	50	400	185 ± 38
			600	-
		100	400	-
			600	12 ± 3

No measurable RIS was found in the Ag/TiO_2 thin film samples.

The best candidates from each plasmonic system were selected. For Au/TiO2, the thin film with 28 at. % of Au, 100 nm of thickness, and annealed at 600 °C revealed a 2.43 ± 0.04 nm LSPR band shift, corresponding to a RIS of 77 ± 1 nm.RIU^{-1}. As for Au-Ag/TiO_2 thin film, the deposition corresponding to approximately 50 nm and a chemical composition of 9 at. % of Au and 8 at. % of Ag (an approximate ratio of 1:1), and annealed at 400 °C with a LSPR band shift of 7.9 ± 0.6 nm, corresponding to a RIS of 250 ± 18 nm.RIU^{-1}.

To mention the big difference of RIS by the addition of Ag to the Au/TiO_2 plasmonic system, plus the bonus of using glass substrates, as the best results for Au-Ag/TiO_2 thin films occurs at 400 °C.

Additionally, a study was performed and published to describe the formation of Au-Ag nanoparticles in the bimetallic plasmonic system. In this work, STEM, STEM-EDX and TEM with *in-situ* annealing were used to describe the formation and growth of these nanoparticles.

2.2 Immobilization of *L. pneumophila* specific biorecognition elements on the surface of the nanocomposite thin films

To produce and immobilize specific biorecognition elements a bibliographic review [30,31] and bioinformatic study of *Legionella pneumophila* whole genome (https://www.ncbi.nlm.nih.gov/nuccore/JFIL01000008.1?report=fasta). From this *L. pneumophila* mip gene was chosen. This gene sequence (Figure 3) is specific to *L. pneumophila* potentiates intracellular infection of protozoa and human macrophages.

5'ATGAAGATGAAATTGGTGACTGCGGCTGTTATGGGGCTTGCAATGTCAACAGCAATGGCTGCAACCGA
TGCCACATCATTAGCTACAGACAAGGATAAGTTGTCTT**[ATAGCATTGGTGCCGATTTGGGGAAGAA]**TTT
TAAAAATCAAGGCATAGATGTTAATCCGGAAGCAATGGCTAAAGGCATGCAAGACGCTATGAGTGGCGC
TCAATTGGCTTTAACCGAACAGCAAATGAAAGACGTTCTTAACAAGTTTCAGAAAGATTTGATGGCAAAG
CGTACTGCTGAATTCAATAAGAAAGCGGATGAAAATAAAGTAAAAGGGGAAGCCTTTTTAACTGAAAACA
AAAACAAGCCAGGCGTTGTTGTATTGCCAAGTGGTTTGCAATACAAAGTAATCAATGCTGGAAATGGTGT
TAAACCTGGTAAATCGGATACAGTCACTGTCGAATACACTGGTCGTCTGATTGATGGTACCGTTTTTGAC
AGTACCGAAAAAACTGGTAAGCCAGCAACTTTTCAGGTTTCACAAGTTATCCCAGGATGGACAGAAGCT
TTGCAATTGATGCCAGCTGGATCAACTTGGGAAATTTATGTTCCCTCAGGTCTTGCATATGGCCCACGTA
GCGTTGGCGGACCTATTGGCCCAAATGAAACTTTAATATTTAAAATTCACTTAATTTCAGTGAAAAAATCA
TCTTAA

Figure 3 – mip gene sequence for *Legionella pneumophila*, with highlighted DNA probe selected to be used as biorecognition element.

From the gene sequence, a single-stranded DNA (ssDNA) primer was design to be used as a biorecognition element for this gene (Figure 3 – grey highlighted area).

Next, the protocol to functionalize the nanoparticles was prepared. Taking in account the well-known interaction between Au nanoparticles and thiol groups, the designed primer was order with a 3' thiol group modification: 5' ATAGCATTGGTGCCGATTTGGGGAAGAA–thiol. Moreover, a complementary ssDNA sequence to the SH-ssDNA primer was also ordered to act as analyte in the next experiments.

Using the T-LSPR detection setup described in section 2.3, immobilization experiments were conducted in Au/TiO_2 thin films annealed at 600 °C. The first experiment consisted in determine, by LSPR band shift, the maximum quantity of ssDNA primer molecules linked to the Au nanoparticles. For this, the microfluidic chamber was filled with Tris-EDTA (TE) buffer and the LSPR signal was measured for 5 min. After this, 0.05 nmol of SH-ssDNA in TE buffer was injected in the microfluidic chamber every 10 minutes. The spectra were analyzed using NANOPTICS software and the results are shown in Figure 4.

The results show a saturation point at around 0.6 nmol of SH-ssDNA in the Au/TiO_2 thin films, as the LSPR signal stabilizes after this amount of DNA probe.

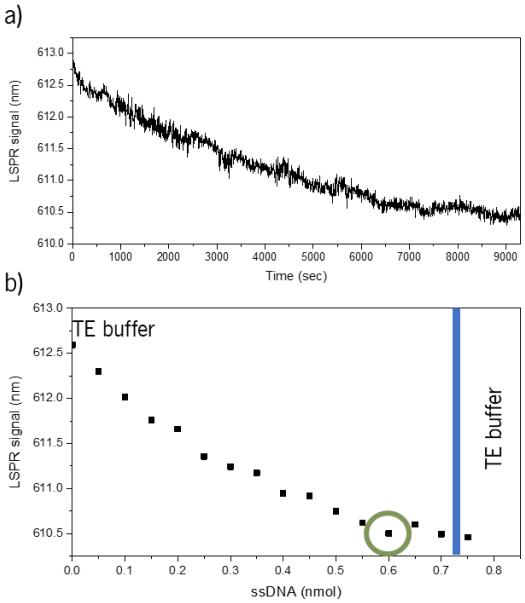

Figure 4 – Results for the first experiment related to the immobilization of the biorecognition elements: a) NANOPTICS analysis of the collected LSPR spectra overtime and b) relation between the LSPR band shift and the amount of the ssDNA immobilized.

After finding this saturation point, the next experiment consisted in adding the complementary ssDNA to a pre-functionalized Au/TiO_2 thin film. The immobilization of SH-ssDNA was performed by adding 0.6 nmol to the microfluidic chamber and let it react for 2 hours while measuring the LSPR signal. After this, TE buffer was injected in the system, followed by 0.1 nmol increments of complementary ssDNA that act as an analyte. As before, the LSPR signal was analyzed using NANOPTICS and the results are presented in figure 5.

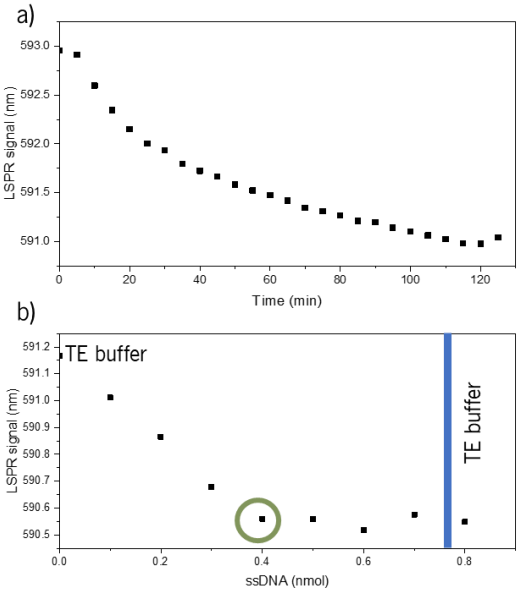

Figure 5 – Results for the second experiment related to the detection of the complementary ssDNA strand: a) immobilization of SH-ssDNA for 2 hours and b) relation between LSPR band shift and amount of complementary ssDNA injected.

The results show that after 0.4 nmol of complementary ssDNA there is a stabilization of the LSPR signal. This may be due to steric impediment between SH-ssDNA molecules bonded to the Au nanoparticle.

The next experiments will consist of the analysis of the LSPR signal after the addition of complementary ssDNA as before but using smaller increments to try and find a finer value for the detection. Smaller increments may also be useful in finding the limit od detection. Moreover, another experiment may be conducted to discern the selectivity of the sensor. This will be performed by using other ssDNA sequences that are not complementary to the biorecognition element.

Finally, the experiments will be repeated for the Au-Ag/TiO_2 thin film samples, to determine if this plasmonic thin film can improve the sensibility of the LSPR detection system for the *L. pneumophila* DNA molecules.

2.3 Preparation of the T-LSPR detection setup for liquid samples.

2.3.1 Microfluidic channel design and production

Keeping in mind the need for miniaturization of the LSPR detection system, microfluidics is to be employed. For this SU-8 molds were created following the design in figure 6, by UV photolithography. After this, the microfluidic channels were produced using polydimethylsiloxane (PDMS). This polymer is a well stablished used in microfluidics and is optically transparent. Following well-established protocols [32], the microfluidic channels are produced by simple methods and without the use of cleanroom facilities.

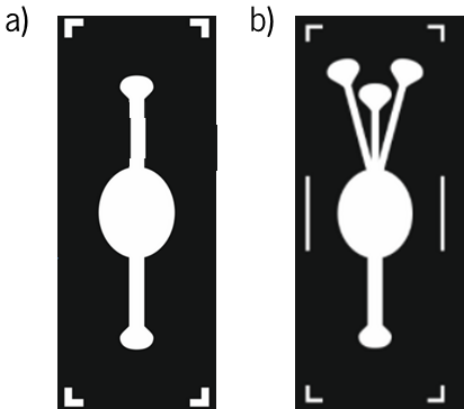

Figure 6 – Microfluidic channel design for the nanoplasmonic detection system with: a) one input and one output; and b) three inputs and one output.

To bond the microfluidic channels to the thin films, O_2 plasma treatment at 30 W for 30 seconds was performed, following an established protocol. However, as it is more difficult to activate TiO_2 in comparison with SiO_2 from glass, a new approach is described in the next subsection

In terms of micropumping, the experiments will be conducted after the assessment of the selectivity and limit of detection of the plasmonic thin films.

2.3.2 Preliminary T-LSPR detection setup

To overcome the difficulties in bonding the microfluidic channels to the thin films, a pressure-based system was designed in SolidWorks software and 3D printed (figure 7). This system as so far assured the correct sealing of the

thin films with the microfluidic channels, by applying constant pressure, and allowed conducting the experiments described in the previous section.

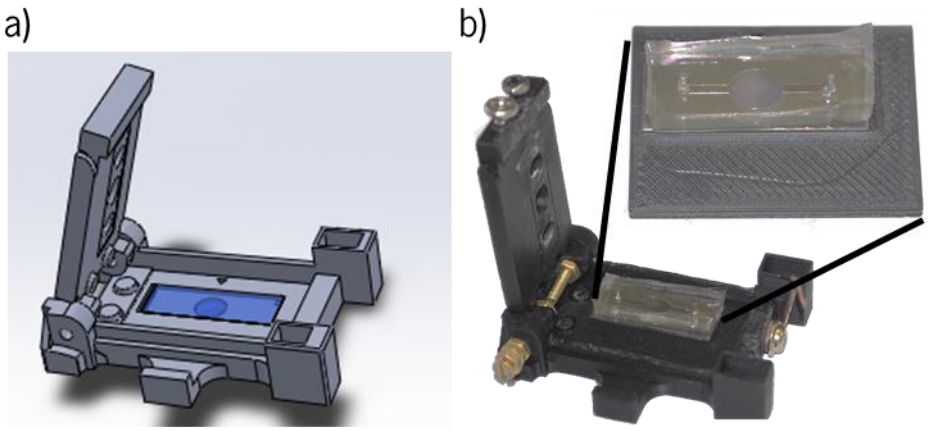

Figure 7 – Thin film and microfluidic channel holder: a) 3D CAD drawing; and b) photographs of the system in use.

To connect the produced sample holder to the LED light source and the modular spectrophotometer and conduct the experiments, a custom-made support was also designed and 3D printed (figure 8). This piece allows to connect fiber optic cables to the light source and spectrophotometer, and also align the light beam inside the sensing chamber.

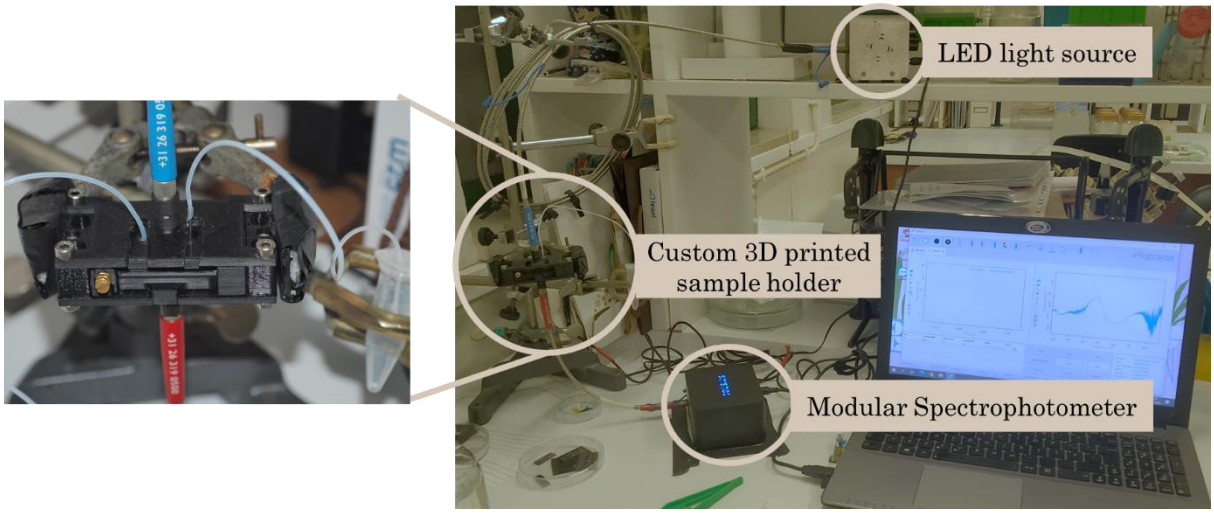

Figure 8 - Prototype of the detection system in use in the CBMA for the immobilization and analyte detection experiments.

This prototype consists of an intermediary step in the construction of the final sensing apparatus and will allow to carry on all the necessary experiments until the integration of all aspects of the final LSPR biosensor system.

Outputs

1. Peer-reviewed articles

D. Costa, J. Oliveira, M.S. Rodrigues, J. Borges, C. Moura, P. Sampaio, F. Vaz, Development of biocompatible plasmonic thin films composed of noble metal nanoparticles embedded in a dielectric matrix to enhance Raman signals, Appl. Surf. Sci. 496 (2019) 143701. https://doi.org/10.1016/j.apsusc.2019.143701

D. Costa, M.S. Rodrigues, L. Roiban, M. Aouine, T. Epicier, P. Steyer, E. Alves, N.P. Barradas, J. Borges, F. Vaz, In-situ annealing transmission electron microscopy of plasmonic thin films composed of bimetallic Au–Ag nanoparticles dispersed in a TiO_2 matrix, Vacuum. 193 (2021). https://doi.org/10.1016/j.vacuum.2021.110511

P. Pereira-Silva, A. Costa-Barbosa, **D. Costa**, M.S. Rodrigues, P. Carvalho, J. Borges, F. Vaz, P. Sampaio, Antifungal activity of ZnO thin films prepared by glancing angle deposition, Thin Solid Films. 687 (2019) 137461. https://doi.org/10.1016/j.tsf.2019.137461

2. Oral Presentations

Costa D., Rodrigues M.S., Borges J., Minas G., Sampaio P., Vaz F. Magnetron sputtered Au:TiO_2 thin films as LSPR-based optical biosensors for DNA samples. VÁCUO 2021 Workshop. Instituto Pedro Nunes, Coimbra, November 9th, 2021

Costa D., Oliveira J., Rodrigues M.S., Borges J., Moura C., Sampaio P., Vaz F. Development of plasmonic thin films composed of noble metal nanoparticles embedded in a dielectric matrix to enhance Raman signals of biomolecules. BRAMAT 2019 11th International Conference on Materials Science & Engineering. Transilvania University of Brasov, Romania, 2019.

Pereira-Silva, P., Costa-Barbosa, A., **Costa, D**., Rodrigues, M.S., Borges, J., Vaz, F. and Sampaio, P. Tailoring the Microstructure of ZnO Thin Films for Antimicrobial Applications. International Conference on Metallurgical Coatings and Thin Films (ICMCTF). San Diego, CA, USA, May 19th to 24th, 2019

3. Posters

Costa, D., Rodrigues, M. S., Roiban, L., Epicier, T., Steyer, P., Borges, J., Vaz, F., Plasmonic response of thin films composed of noble metal nanoparticles dispersed in dielectric matrixes, ICTF-JVC 2020, 23-26 November 2020

Costa, D., Rodrigues, M. S., Roiban L., Steyer P., Borges J., Vaz F., Influence of nanoparticle size and composition on the plasmonic response of Au-TiO_2 and Au/Ag-TiO_2 thin films. Jornadas do CF-UM-UP 2019, Universidade do Minho, Campus de Gualtar, 13 de dezembro 2019.

4. Awards

IUVSTA-ELSEVIER STUDENT AWARD / ICTF-JVC 2020, Budapest, Hungary

18th International Conference on Thin Films & 18th Joint Vacuum Conference Student Award to attend the conference with the abstract: "Plasmonic response of thin films composed of noble metal nanoparticles dispersed in dielectric matrixes"

5. Courses

6th Introduction to data analysis and image processing with MATLAB - May 4th-7th, 2020, Instituto de Investigação e Inovação em Saúde (I3S) - Universidade do Porto

Bibliography

[1] A. Assaidi, M. Ellouali, H. Latrache, et al., Adhesion of Legionella pneumophila on glass and plumbing materials commonly used in domestic water systems, Int. J. Environ. Health Res. 3123 (2018) 1–9.

[2] M. Sabria, and V.L. Yu, Hospital-acquired legionellosis: Solutions for a preventable infection, Lancet Infect. Dis. 2 (2002) 368–373.

[3] N. Párraga-Niño, S. Quero, N. Uria, et al., Antibody test for Legionella pneumophila detection, Diagn. Microbiol. Infect. Dis. 90 (2018) 85–89.

[4] J.F. Plouffe, T.M. File, R.F. Breiman, et al., Reevaluation of the definition of legionnaires' disease: Use of the urinary antigen assay, Clin. Infect. Dis. 20 (1995) 1286–1291.

[5] R. Hase, K. Miyoshi, Y. Matsuura, et al., Legionella pneumonia appeared during hospitalization in a patient with hematological malignancy confirmed by sputum culture after negative urine antigen test, J. Infect. Chemother. (2018) 10–13.

[6] P. Poltronieri, M.D. De Blasi, and O.F. D'Urso, Detection of Listeria monocytogenes through real-time PCR and biosensor methods, Plant, Soil Environ. 55 (2009) 363–369.

[7] D.R. Willett, and G. Chumanov, LSPR Sensor Combining Sharp Resonance and Differential Optical Measurements, Plasmonics. 9 (2014) 1391–1396.

[8] B. Sepúlveda, P.C. Angelomé, L.M. Lechuga, et al., LSPR-based nanobiosensors, Nano Today. 4 (2009) 244–251.

[9] A.J. Haes, and R.P. Van Duyne, A unified view of propagating and localized surface plasmon resonance biosensors, Anal. Bioanal. Chem. 379 (2004) 920–930.

[10] C. Huang, K. Bonroy, G. Reekmans, et al., Localized surface plasmon resonance biosensor integrated with microfluidic chip, Biomed. Microdevices. 11 (2009) 893–901.

[11] M. Estevez, M.A. Otte, B. Sepulveda, et al., Trends and challenges of refractometric nanoplasmonic biosensors: A review, Anal. Chim. Acta. 806 (2014) 55–73.

[12] S.S. Aćimović, M.A. Ortega, V. Sanz, et al., LSPR chip for parallel, rapid, and sensitive detection of cancer markers in serum, Nano Lett. 14 (2014) 2636–2641.

[13] J.N. Anker, W.P. Hall, O. Lyandres, et al., Biosensing with plasmonic nanosensors., Nat. Mater. 7 (2008) 442–53.

[14] I. Doron-Mor, H. Cohen, Z. Barkay, et al., Sensitivity of transmission surface plasmon resonance (T-SPR) spectroscopy: Self-assembled multilayers on evaporated gold Island films, Chem. - A Eur. J. 11 (2005) 5555–5562.

[15] M. Lahav, A. Vaskevich, and I. Rubinstein, Biological sensing using transmission surface plasmon resonance spectroscopy, Langmuir. 20 (2004) 7365–7367.

[16] G. Cappi, F. Spiga, and Y. Moncada, Label-Free Detection of Tobramycin in Serum by Transmission-Localized Surface Plasmon Resonance, Anal. .... (2015).

[17] I. Ruach-Nir, T.A. Bendikov, I. Doron-Mor, et al., Silica-stabilized gold island films for transmission localized surface plasmon sensing, J. Am. Chem. Soc. 129 (2007) 84–92.

[18] M.S. Rodrigues, J. Borges, C. Gabor, et al., Functional behaviour of TiO_2 films doped with noble metals, Surf. Eng. 32 (2015) 1743294415Y.000.

[19] J. Borges, D. Costa, E. Antunes, et al., Biological behaviour of thin films consisting of Au nanoparticles dispersed in a TiO_2 dielectric matrix, Vacuum. 122 (2015) 1–9.

[20] J. Borges, M.S. Rodrigues, T. Kubart, et al., Thin films composed of gold nanoparticles dispersed in a dielectric matrix: The influence of the host matrix on the optical and mechanical responses, in: Thin Solid Films, 2015: pp. 8–17.

[21] J. Borges, M.S. Rodrigues, C. Lopes, et al., Thin films composed of Ag nanoclusters dispersed in TiO_2: Influence of composition and thermal annealing on the microstructure and physical responses, Appl. Surf. Sci. 358 (2015) 595–604.

[22] J. Borges, T. Kubart, S. Kumar, et al., Microstructural evolution of Au/TiO_2 nanocomposite films: The influence of Au concentration and thermal annealing, Thin Solid Films. (2015).

[23] J. Borges, M. Buljan, J. Sancho-Parramon, et al., Evolution of the surface plasmon resonance of Au:TiO_2 nanocomposite thin films with annealing temperature, J. Nanoparticle Res. 16 (2014) 2790.

[24] M.S. Rodrigues, D. Costa, R.P. Domingues, et al., Optimization of nanocomposite Au/TiO_2 thin films towards LSPR optical-sensing, Appl. Surf. Sci. (2017).

[25] G.A. Lopez, M.C. Estevez, M. Soler, et al., Recent advances in nanoplasmonic biosensors: Applications and lab-on-a-chip integration, Nanophotonics. 6 (2017) 123–136.

[26] W.P. Hall, S.N. Ngatia, and R.P. Van Duyne, LSPR biosensor signal enhancement using nanoparticle-antibody conjugates, J. Phys. Chem. C. 115 (2011) 1410–1414.

[27] J.-H. Park, J.-Y. Byun, W.-B. Shim, et al., High-sensitivity detection of ATP using a localized surface plasmon resonance (LSPR) sensor and split aptamers., Biosens. Bioelectron. 73 (2015) 26–31.

[28] A.H. Nguyen, and S.J. Sim, Nanoplasmonic biosensor: detection and amplification of dual bio-signatures of circulating tumor DNA., Biosens. Bioelectron. 67 (2015) 443–9.

[29] M.S. Rodrigues, R.M.S. Pereira, M.I. Vasilevskiy, et al., NANOPTICS: In-depth analysis of NANomaterials for OPTICal localized surface plasmon resonance Sensing, SoftwareX. 12 (2020) 100522.

[30] G. Qiu, Z. Gai, Y. Tao, et al., Dual-Functional Plasmonic Photothermal Biosensors for Highly Accurate Severe Acute Respiratory Syndrome Coronavirus 2 Detection, ACS Nano. 14 (2020) 5268–5277.

[31] X. Ma, Y. Li, Y. Liang, et al., Development of a DNA microarray assay for rapid detection of fifteen bacterial pathogens in pneumonia, BMC Microbiol. 20 (2020) 1–13

[32] V.C. Pinto, P.J. Sousa, V.F. Cardoso, et al., Optimized SU-8 processing for low-cost microstructures fabrication without cleanroom facilities, Micromachines. 5 (2014) 738–755.